

P. BALLEYGUIER, R. DEI-CAS, S. JOLY, H. LEBOUTET

Commissariat à l'Energie Atomique  
 Service de Physique et Techniques Nucléaires  
 B.P. n° 12  
 91680 BRUYERES-LE-CHATEL. FRANCE

Abstract

For the acceleration of a high-brightness high-peak power electron beam, an accelerating chain at 433 MHz has been developed. A mock-up of a 3-cell cavity has been built to study mainly the effects the electron beam could sustain with respect to energy spread and emittance growth which are of crucial importance for the FEL application. The following measurements have been performed with an optimized cell geometry : i) E-field distribution in the three cells related to the definition of the coupling slots and ii) higher order mode distribution related the design of efficient dampers. Piston tuners for the resonance frequency adjustment as well as the RF feeding loop have also been studied with this mock-up.

Introduction

High quality beams with high peak current can be transported by using a low-frequency linac. For the ELSA FEL, presently in the building phase at Bruyères-le-Châtel [1,2], we have developed a 433 MHz accelerator chain.

We report here on the work done on a 3-cell full-scale mock-up to define the cell geometry as well as the couplers and tuners.

In a 3-cell cavity, we define the coupling coefficient as :

$$\gamma = 2 \frac{f_{\pi/3} - f_{\pi}}{f_{\pi/3} + f_{\pi} \cos \pi/3}$$

where  $f_{\pi}$ ,  $f_{2\pi/3}$  and  $f_{\pi/3}$  are the frequencies of the three  $TM_{010}$  modes of the 3-cell cavity.

The geometrical impedance is defined by :

$$g = R/Q = \frac{1}{2PQ} \left| \int E_z e^{i\omega z/c} dz \right|^2$$

where P is the power dissipated in the cavity walls.

The normalized electric field is :

$$\tilde{E}_z = E_z \sqrt{\epsilon_0 / 2W}$$

where W is the energy stored in the cavity.

The linac under construction is a standing-wave accelerator with cavities operating in the  $\pi$ -mode. The 433 MHz 3-cell cavities have an unloaded Q of 35000 with an input peak power of about 2 MW ; the coupling between cells is made by means of 6 slots per disk resulting in a coupling factor larger than 1.3 %.

The full-sized mock-up was made modular to allow both 1-cell or 3-cell configurations (fig. 1).

A good quality factor ( $\sim 25000$  for a 1-cell cavity) has been achieved on the mock-up by brushing over the joints with silver lake.

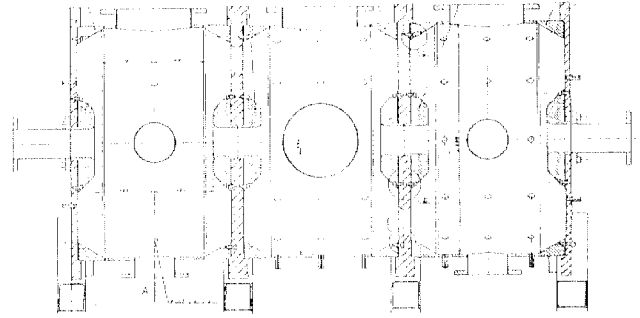


Fig. 1 - 3-cell configuration of the cavity mock-up.

Cell coupling

Initially, the coupling coefficient was too low. Consequently, the coupling slots have been enlarged to increase it as shown in figure 2. The initial slot area (4235 mm<sup>2</sup>) has been increased to 6158 mm<sup>2</sup> (increase ratio of 1.45) resulting in an increase of the coupling factor from 0.56 % to 1.65 %, respectively. The coupling coefficient increase (2.80) is somewhat higher than the expected value (2.10), based on a simulation with the 2D URMEL code.

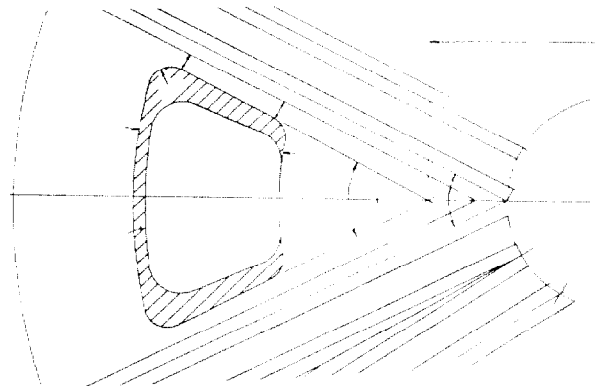


Fig. 2 - Shapes of coupling slots.

In this simulation, we used the  $TE_{111}$  mode of a two-cell cavity (figure 3), to test how the coupling coefficient would vary as a function of the dimensions (diameter, thickness) of the coupling hole. The result was that the coupling coefficient is proportional to the square of the coupling hole area (i.e. the fourth power of its diameter), and decreases exponentially with the thickness of the coupling disc ; the decay constant is equal to the field decay constant in a circular wave guide of the same diameter than the coupling hole.

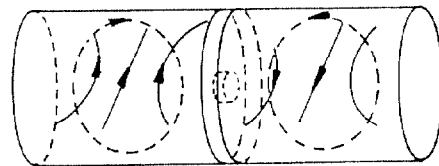


Fig. 3 -  $TE_{111}$  mode in a 2-cell cavity.

**Field measurements**

The normalized electric field has been measured using the perturbation technique. The geometrical impedance of the accelerating mode has been computed from these measurements (figure 4), and found to be approximately three times the value computed with URMEL (129.6 Ω) for a single-cell cavity. The perturbation object was a steel needle 1.1 mm in diameter and 19 mm long. The cavity has been previously adjusted to have equal fields in the three cells, as achieved by using the one-third criterion [3] :

$$\frac{f_{2\pi/3} - f_{\pi}}{f_{\pi/3} - f_{\pi}} = \frac{1}{3}$$

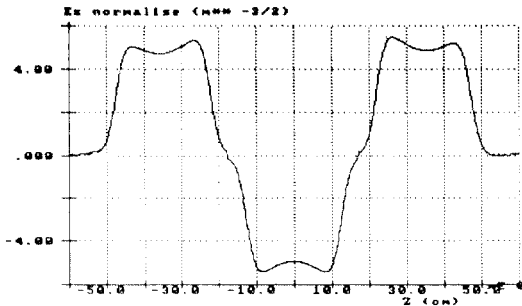


Fig. 4 - Field distribution of the accelerating mode.  
f = 433.33 MHz      g = 391.7 Ω

We also measured the field asymmetry due to the piston tuner in a single-cell cavity. The measurement was made along two paths, parallel to the axis (at 25 mm from it), in the tuner direction and in the opposite direction [4] .

With our system, based on a phase-locked loop to measure the frequency shift caused by the perturber, the frequency resolution was 10 Hz and the noise level about 30 Hz, for a typical shift of 35 kHz in the middle of the cavity. The measurement duration was about one minute. With such values, we absolutely had to take into account the thermal shift of the frequency.

In a first experiment, it has been found that the difference of g-values measured for both paths, was not higher than the dispersion of these measurements. This reproductibility default was caused by measuring the field in the beam pipe, at the cavity ends where the field is small. This is due to the principle of the perturbation technique : since the frequency shift is proportional to the square of the field value, a small frequency error leads to a quite high field relative error when it is small. To improve the reproductibility, we decided to fit both the extreme parts of the measured curve with an exponential function, according to the theoretical field in a circular waveguide below the cutoff frequency. This mathematical treatment allowed us to reduce the dispersion by a factor of three (table 3).

One can show that the equivalent displacement Δy of the electrical cavity center is related to the difference of g-values for both paths by :

$$\Delta y = \left(\frac{c}{\omega}\right) \frac{21}{h} \frac{\Delta g}{g}$$

Geometrical impedance measurements have been performed in both paths separated by h = 50 mm (figure 5 and table 1). The tuner diameter was 145 mm, and his penetration inside the cavity was 16 mm. The resulting value of Δy = 1.7 mm is unacceptable. For that reason, it has been decided that there would be two tuners per cell, diametrically opposed, to compensate their asymmetrical effects.

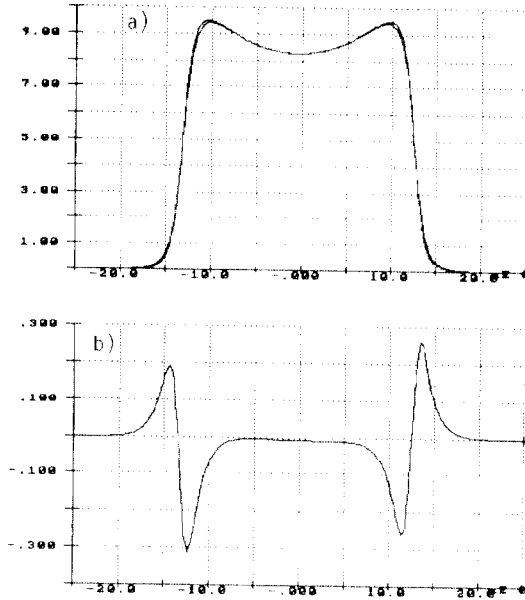


Fig. 5 - Field asymmetry due to a tuner ; along both paths (a) and difference (b)

**Table 1** - Measurement of geometrical impedance asymmetries

	fit	g (Ω)		Δg (Ω)	Δy (mm)
		in plunger direction	in opposite direction		
number of measurements		6	5		
mean value	no	126.156	126.956	0.800	1.53
dispersion		0.077	0.096	0.123	0.24
mean value	yes	126.364	127.235	0.871	1.67
dispersion		0.025	0.039	0.046	0.09

**Higher order mode (HOM) measurements**

HOM geometrical impedances have been measured in a single-cell cavity, up to 2 GHz for monopole modes and up to 1 GHz for dipole modes. The results are in very good agreement with URMEL computations.

In the 3-cell configuration, HOM identification has been tried around several frequencies obtained from URMEL calculations. Around 1.6 GHz, we observed that hybrid coupling between different modes could occur (figure 6). The perturbation object was a copper sphere of 6 mm in diameter. Positive frequency shift is due to magnetic field and negative shift to electric field.

HOM dampers have been developed (figure 7). The experiments showed that dampers with a coupling loop could damp both even and odd modes. So, two orthogonally placed devices per cell should damp most of the parasitic modes. Of course, such dampers must include a stop-band filter at the accelerating frequency, and terminated by a short-circuit. Tuning is obtained by adjusting the inner tube length ; a rejection of 60 dB has been achieved. The efficiency of these dampers, in a single-cell cavity, is shown in table 2, for the most dangerous modes. These results have to be taken with care, because of great difficulties in identifying damped modes.

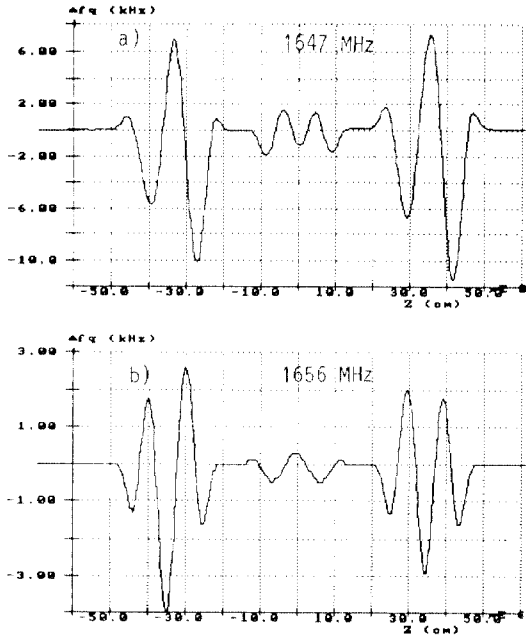


Fig. 6 - Hybrid coupling of  $TM_{122}$  and  $TM_{113}$  modes ;  $TM_{122}$  in outer cells,  $TM_{113}$  in inner cell (a) and  $TM_{113}$  in outer cells,  $TM_{122}$  in inner cell (b).

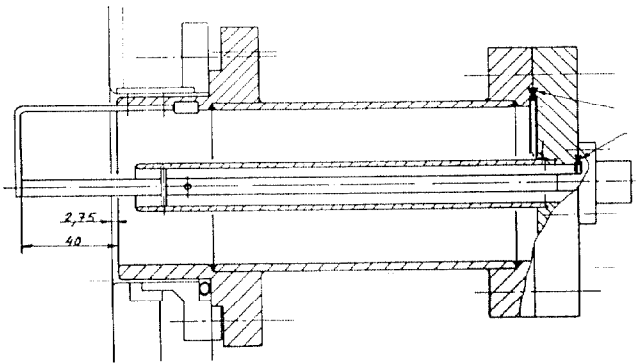


Fig. 7 - HOM damper.

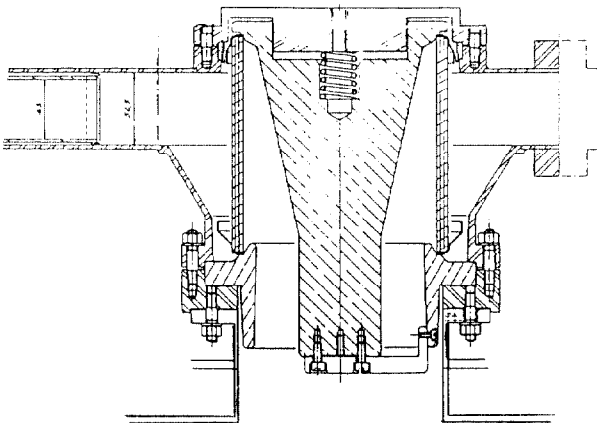


Fig. 8 - Power injection loop.

Table 2 - HOM damping in a single-cell cavity

mode	no damper		1 damper		2 orthogonal dampers	
	f(MHz)	Q	f(MHz)	Q	f(MHz)	Q
TM010	440.0	23700	440.0	23700	439.7	22600
TM011	646.4	25300	645.9	3000	645.3	950
TM021	1162.6	23000	1160.0	1050	1159.1	900
TM022	1450.6	20500	1459.7	900	1459.0	300
TM110	748.1	37400	748.4	32800	*748.7	1800
	748.5	32800	748.8	2200		
TM111	931.6	27400	925.9	230	922.4	150
	931.8	28200	931.6	28300	930.2	1000
TM112	1271.8	35600	1272.7	30000	1272.0	24000
	1272.8	33300	1272.3	35200	1237.5	5100
TM121	1355.2	21100	1355.3	5700	1349.8	400
	1355.6	25600	1355.1	15500	1352.9	4600
TM122	*1648.5	18400	1647.8	1900	1648.4	1200
			1648.3	10000	1649.8	7500

\* (both polarizations overlap)

Power injection loop

The injection loop had been designed to allow high power input. For that reason, its dimensions are rather large. The loop is constituted of a short-circuit between both conductors at the end of a coaxial structure with diameters of 60 mm and 127 mm. Consequently, the coupling factor  $\beta$  tends to be large and the short-circuit has to be pushed back inside the injection part at 50 mm from the cavity sleeve to lower the  $\beta$ -value down to 2, which is the required value without beam (figure 8). The voltage node position has been determined by measuring the phase difference between incident and reflected signals. This value was compared with that obtained after substituting the bar by a short-circuit disc. Then, the voltage node was found to be at about 12 cm from the bar, i.e. near the center of the insulator.

Conclusion

This mock-up allowed us to measure most of the parameters a 2D code could not calculate ; cell coupling, HOM damping, injection loop coupling, plunger characteristics, ... We also discovered that hybrid coupling (one mode in one cell, and another mode in an adjacent cell) could occur. All these results have been helpful to design the actual ELSA cavities. The authors thank A. Bloquet for measurements.

References

[1] R. Dei-Cas et al., "Photo-injector, accelerator chain and wiggler development programs for a high peak power RF free electron laser" FEL-89, Nucl. Instr. Meth. A 285 (1989) 320-326.

[2] R. Dei-Cas et al., "Status report on the low-frequency photo-injector and on the infrared FEL experiment (ELSA)", to be presented at FEL-90.

[3] P. Balleyguier, to be published in Nucl. Instr. Meth. A

[4] A. Wetter and R. Friedman, "Measurements of Field asymmetry in accelerating cavities with waveguide couplers", Linac-88.